Wilber, W. J., & Lipman, D. (1983) *Proc. Natl. Acad. Sci. U.S.A. 80*, 726–730.
Yokoyama, S., Oobayashi, A., Tanabe, O., & Ichishima, E. (1975) *Biochim. Biophys. Acta 397*, 434–448.
Yoon, M. Y., & Cook. P. F. (1987) *Biochemistry 26*, 4118–4125.
Young, M., Sammons, R. D., Mueller, W. T., & Benkovic, S. J. (1984) *Biochemistry 23*, 3979–3986.
Young, M., Wasserman, G., Benkovic, P., & Benkovic, S. J. (1985) in *Proceedings of the Second Workshop on Folyl and Antifolylpolyglutamates* (Goldman, I. D., Ed.) pp 76–90, Praeger, New York.

Zinc Interactions with Regulatory Dimers from *Escherichia coli* Aspartate Transcarbamoylase†

John R. Jefferson,‡ John B. Hunt,§ and Ann Ginsburg*
Section on Protein Chemistry, Laboratory of Biochemistry, National Heart, Lung, and Blood Institute, National Institutes of Health, Bethesda, Maryland 20892

Received July 25, 1989; Revised Manuscript Received March 28, 1990

ABSTRACT: Zn^{2+} is tetrahedrally bonded to the 4 nonadjacent thiols of each regulatory chain (M_r 17 000) near r–c contacts between catalytic (c) and regulatory chains (r) in aspartate transcarbamoylase (ATCase; c_6r_6). This paper reports on Zn^{2+} interactions with r dimer in the absence of stabilizing r–c contacts. After r_2 and c_3 subunits were separated, –SH groups of r_2 were titrated with *p*-(hydroxymercuri)benzenesulfonate (PMPS) at pH 7.0. The concomitant release of Zn^{2+} (2 equiv/r dimer) was quantitated with 4-(2-pyridylazo)resorcinol (PAR) and was a linear function of PMPS added until 8 mercaptide bonds per r_2 were formed. Breakage of 1 of 4 Zn^{2+}–sulfur bonds in a Zn^{2+} binding cluster therefore makes the other three bonds more labile. From stopped-flow measurements, the PMPS-promoted Zn^{2+} release from r_2 or mercaptide bond formation with 10- to 20-fold excess PMPS/r_2–SH at pH 7.0 was first order with an Arrhenius activation energy E_a = 10 kcal/mol and a half-time $t_{1/2}$ = 9 ± 2 ms at 20 °C without inhibitory anions present. The rate of mercurial-promoted Zn^{2+} release from r_2 is at least 77 times faster than that from intact c_6r_6 [Hunt, J. B., Neece, S. H., Schachman, H. K., and Ginsburg, A. (1984) *J. Biol. Chem. 259*, 14793]; this indicates that Zn^{2+} binding clusters are more accessible to attack by PMPS than are those in ATCase. The addition of a 25-fold excess of the multidentate fluorescent chelator quin-2 to r_2 gave a rate of Zn^{2+} dissociation that was 1/210th of that observed with excess mercurial. Furthermore, the $Zn(PAR)_1$ complex was identified as the active species in the transfer of Zn^{2+} from $Zn(PAR)_2$ to aporegulatory subunits, with $k = (8 \pm 3) \times 10^5$ M^{-1} s^{-1} at pH 7.0 and 15 °C for this second-order association reaction. Although kinetic results are dependent on the mechanisms involved, an affinity constant $K'_A = (1.3 \pm 0.6) \times 10^{12}$ M^{-1} for Zn^{2+} binding to r dimer at pH 7.0 and 20 °C in the absence and presence of 100 mM KCl could be determined spectrally by rapid equilibration with the high-affinity, sensitive metalloindicators indo-1 and quin-2. This K'_A value is based on the assumptions that Zn^{2+} binding sites in r_2 are equivalent (noninteracting) and that apo-r_2 does not dissociate; if apo-r_2 dissociates, $K'_A \approx 10^{14}$ M^{-1}. Within experimental error, the K'_A value was independent of [indo-1]/[r_2] ratios from 36 to 3 with 0.3–8 μM r_2. Thus, $\Delta G' \simeq -16$ kcal/mol at 20 °C (pH 7.0) for sequential formation of 4 Zn^{2+}–thiol bonds (inclusive of energy changes for polypeptide chain transitions). CTP (1 mM ± 1 mM Mg^{2+}) and Mg·ATP (1 mM) increased $K'_A \leq \sim 1.2$- and ~1.7-fold, respectively, for r_2 binding Zn^{2+}.

A goal of studying Zn^{2+} interactions with aspartate transcarbamoylase (ATCase)[1] from *Escherichia coli* (EC 2.1.3.2) and with isolated regulatory subunits of ATCase is to gain information on the structural roles of Zn^{2+} in the intact enzyme and in the assembly of ATCase. Assembly processes and protein–protein interactions depend on the correct folding of polypeptide chains, and Zn^{2+} binding to the four nonadjacent Cys residues of each regulatory chain will restrict folding pathways and constrain the final conformations assumed. Recently, the Zn^{2+} domain of each regulatory chain of ATCase was shown to be homologous with the "Zn finger" structure of transcriptional factor IIIA from immature oocytes of *Xenopus laevis* (Berg, 1988), which is the first discovered example of an important class of DNA-binding proteins containing tandem repeats of "Zn finger" structural motifs for

† Presented in part at the 1987 meeting of the American Society of Biological Chemists, Philadelphia, PA (Jefferson et al., 1987), and at the 1988 FASEB meeting in Las Vegas, NV (Jefferson et al., 1988).

* Correspondence should be addressed to this author at NHLBI, NIH, Building 3, Room 208, Bethesda, MD 20892.
‡ Present address: College of Pharmacy, University of Cincinnati, Cincinnati, OH 45267-004.
§ Present address: National Science Foundation, 1800 G Street, N.W., Washington, DC 20550.

[1] Abbreviations: ATCase or c_6r_6, aspartate transcarbamoylase; c_3, catalytic trimer subunit; r_2, regulatory dimer subunit containing 2 equiv of specifically bound Zn^{2+} unless designated as apo-r_2; PAR, 4-(2-pyridylazo)resorcinol; indo-1, 1-[2-amino-5-(6-carboxyindol-2-yl)phenoxy]-2-(2′-amino-5′-methylphenoxy)ethane-*N,N,N′,N′*-tetraacetic acid; quin-2, 2-[[2-[bis(carboxymethyl)amino]-5-methylphenoxy]methyl]-6-methyl-8-[bis(carboxymethyl)amino]quinoline; PMPS, *p*-(hydroxymercuri)benzenesulfonate; neohydrin, 1-[3-(chloromercuri)-2-methoxypropyl]urea; 2-ME, 2-mercaptoethanol; Hepes, 4-(2-hydroxyethyl)-1-piperazineethanesulfonic acid.

DNA recognition (Miller et al., 1985; Klug & Rhodes, 1987). Techniques developed for studies of Zn^{2+} interactions with ATCase (Hunt et al., 1984, 1985) and with regulatory subunits of ATCase (reported here) have used high-affinity, sensitive, metallochelator indicators. These methods currently are being applied to studies of Zn^{2+}-dependent structures of transcriptional factor IIIA (Han et al., 1989, 1990).

Each molecule of ATCase from *E. coli* contains six Zn^{2+} ions, which have an essential role in maintaining the quaternary structure of this allosteric enzyme (Nelbach et al., 1972; Rosenbusch & Weber, 1971a,b). The enzyme contains six c and six r chains, structurally arranged as two superimposed trimers of c chains bridged noncovalently by three r chain dimers (Weber, 1968; Rosenbusch & Weber, 1971a; Meighen et al., 1970; Cohlberg et al., 1972; Monaco et al., 1978; Honzatko et al., 1982; Kantrowitz & Lipscomb, 1988). Each Zn^{2+} ion is tetrahedrally bonded to the four Cys residues of each r chain (residues 109, 114, 138, and 141) near the region of contact between r and c chains (Kim et al., 1987). ATCase exhibits positive cooperativity in catalysis (Gerhart & Pardee, 1962; Gerhart, 1970), and CTP acts as an allosteric inhibitor whereas ATP is an allosteric activator. The allosteric effectors bind to the N-terminal domain, and the Zn^{2+} domain is near the C-terminal of each r chain (Monaco et al., 1978; Kim et al., 1987).

Dimers of isolated regulatory chains are stabilized by Zn^{2+} binding to the extent that there is no apparent dissociation of r dimers (at >0.09 g/L) containing 1 equiv of Zn^{2+}/r chain, and only metalloregulatory chain dimers are competent to associate with catalytic chain trimers in ATCase assembly (Cohlberg et al., 1972). However, EDTA-treated aporegulatory subunits of ATCase were observed to exist in a monomer–dimer equilibrium with nonparticipating higher aggregates (Cohlberg et al., 1972). Nevertheless, the sensitivity of Zn^{2+} binding thiol clusters of r chains to oxidation makes it difficult to characterize aporegulatory subunits.

This paper describes some aspects of Zn^{2+} interactions with isolated regulatory dimers of ATCase. Some advantages and limitations of using metallochelator indicators in kinetic studies of Zn^{2+} release and uptake are discussed.

Materials and Methods

Protein Preparations. ATCase from *E. coli* was kindly provided by Ying R. Yang and Howard K. Schachman, University of California at Berkeley, and was stored at 4 °C as a concentrated suspension (8–15 mg/mL) in 3.6 M $(NH_4)_2SO_4$, pH 7.0, containing 5 mM 2-ME. The Zn^{2+} content by atomic absorption analyses was 6.0 ± 0.2 equiv of Zn^{2+}/mol of ATCase. Regulatory and catalytic subunits were isolated from ATCase following the procedure of Yang et al. (1978) using buffers that had been thoroughly degassed. Briefly, 20 mg of ATCase was collected from the ammonium sulfate suspension by centrifugation and dissolved in 2 mL of 10 mM Tris·HCl/100 mM KCl, pH 8.7 (25 °C), and dialyzed at 4 °C against two 500-mL portions of the same buffer over an 18-h period. The protein was recovered from the dialysis bag and treated with a 10-fold excess of neohydrin/–SH for 2 h at room temperature. The sample then was loaded onto a column of DE-52 (Whatman, 1 × 28 cm) which had been equilibrated with the dialysis buffer at 4 °C and was eluted with the same buffer. The first fractions absorbing at 280 nm contained the regulatory subunits, and these were pooled and immediately made 10 mM in 2-ME and then 0.2 mM in Zn^{2+}. The pooled fractions were dialyzed overnight at 4 °C against 1 L of 25 mM Tris·HCl, pH 8.0 (25 °C), 2 mM 2-ME, and 0.2 mM Zn^{2+}, followed by dialysis against 1 L of 3.6 M $(NH_4)_2SO_4$, pH 7.0, containing 2 mM 2-ME at 4 °C for 24 h. The protein was recovered from the dialysis bag, pelleted by centrifugation, and resuspended in a small plastic microtube in 500 μL of the final dialysate, yielding ~10 mg of r_2/mL of $(NH_4)_2SO_4$ suspension. Regulatory subunits were stable in $(NH_4)_2SO_4$ suspensions at 4 °C for 1–2 weeks, provided that air was excluded as much as possible by degassing buffers and minimizing surface–air contact. The catalytic subunits from the neohydrin-treated ATCase were recovered also from the DE-52 column by changing the elution buffer to 10 mM Tris·HCl, pH 8.7 (25 °C), with 500 mM KCl. Fractions containing the catalytic subunits eluted as a large UV-absorbing peak (280 nm) just after a very small sharp peak of undissociated ATCase. The pooled fractions containing c_3 were treated with 10 mM 2-ME and dialyzed overnight at 4 °C against 1 L of 3.6 M $(NH_4)_2SO_2$ (pH 7.0) containing 5 mM 2-ME. The suspension of catalytic subunits was then recovered from the dialysis bag, pelleted by centrifugation, and resuspended with 500 μL of the dialysis buffer, yielding ~20 mg of c_3/mL of $(NH_4)_2SO_4$ suspension. Catalytic subunits usually were stable in $(NH_4)_2SO_4$ suspensions at 4 °C, but occasionally these isolated subunits were inactive in ATCase assembly experiments and had to be discarded.

Protein concentrations were determined from published absorption coefficients (cm^2 mg^{-1}) at 280 nm: $A^{0.1\%} = 0.59$ for ATCase (Blackburn & Schachman, 1976); $A^{0.1\%} = 0.72$ for c_3 subunit and 0.30 for r_2 subunit (Yang et al., 1978). It often was necessary to correct the apparent A_{280nm} of r_2 for light scattering, and that was approximated by subtracting from the observed A_{280nm} a value obtained at 280 nm from a linear extrapolation of the sample absorbance from 340 to 310 nm (where the protein does not absorb light). Regulatory and catalytic subunit preparations were analyzed by UV absorbance spectra and by evaluating their competency to associate in ATCase assembly (Nelbach et al., 1972; Cohlberg et al., 1972), as monitored by polyacrylamide gel electrophoresis under nondenaturing conditions (Hunt et al., 1985).

Free and/or loosely bound Zn^{2+} in each r_2 preparation (≤27% of total Zn^{2+}) was measured from the absorbance increase at 500 nm when r_2 was added to a solution of 10^{-4} M PAR at pH 7.0 and 20 °C ($\Delta\epsilon = 6.6 \times 10^4$ M^{-1} cm^{-1}; Hunt et al., 1985). Then, excess PMPS/–SH groups present was added, and the mercurial-promoted Zn^{2+} release from r_2 was calculated from the ΔA_{500nm} value. The latter gave a quantitative measure of native r dimer. Excess 2-ME/PMPS present was added next to displace PMPS from r_2, and the decrease in A_{500nm} gave a measure of Zn^{2+} rebinding to r_2 (≥80%).

For stopped-flow experiments (with the exception of those shown in Figure 2 below) and for spectral measurements, solutions of regulatory subunits were prepared at 4 °C by dissolving ~3 mg of protein obtained by centrifugation of the $(NH_4)_2SO_4$ suspension (see above) in the desired buffer (100 μL) and passing this solution through a Bio-Rad P-10 (100–200 mesh) column (0.75 × 24 cm) equilibrated with degassed buffer. The UV absorbing (280-nm) fractions were collected so as to minimize the dilution of r_2 and to maximize the separation of r_2 from $(NH_2)_2SO_4$ and 2-ME. For preparation of the PMPS adduct of Zn^{2+}-free r_2, an excess of PMPS/–SH groups was added to r_2, and then this solution was passed through a Chelex 100 (K^+ form) column (~1 × 18 cm), which was equilibrated with the desired buffer, to remove free Zn^{2+} and free PMPS. For preparation of aporegulatory subunits, the Chelex 100 eluate of the r_2–$(PMPS)_8$ adduct was treated immediately with excess 2-ME, and then

the apoprotein was gel filtered through a P-10 column (as above) to remove 2-ME and the mercurial adduct of 2-ME. The aporegulatory subunits were used as soon as possible after elution from the P-10 column, since there was a substantial decline in their ability to bind Zn^{2+} over 24 h. The susceptibility of r_2 sulfhydryl groups to oxidation appears to be a major factor in the instability of apo-r_2.

Chemicals. Water, which was distilled and then deionized and filtered through a Millipore Milli-Q2 reagent-grade system, was used for rinsing glassware and for preparing solutions. All buffers were purified by passage through a column (5 × 37 cm) of Chelex 100 resin (100–200 mesh) obtained from Bio-Rad and regenerated in the K^+ form, after which Zn^{2+} could not be detected by atomic absorption measurements ($<10^{-8}$ M Zn^{2+}). The pH measurements of buffers were made at 20 °C using pH 6.881 and 4.002 reference buffers (Leeds and Northrup, 103002 and 103001, respectively) equilibrated at this temperature. Bovine pancreatic RNase A was purchased from Worthington. Solid PMPS and *N*-acetyl-L-tryptophanamide (Sigma) were stored desiccated at −20 °C. Stock solutions of PMPS (5 mM) were stored at 4 °C for no longer than 1 week, and their concentrations were checked by spectrophotometric titration at 250 nm with standard solutions of glutathione (Boyer, 1954). Stock solutions (about 0.1 M) of ATP (Sigma) and CTP (from Boehringer-Mannheim) were prepared by dissolving the solids in water at 2 °C and adjusting the pH to 7.0 with dilute KOH. Concentrations were determined spectrophotometrically ($\epsilon_{259nm} = 15.4 \times 10^3$ for ATP and $\epsilon_{271nm} = 9.0 \times 10^3$ M^{-1} cm^{-1} for CTP), and the solutions were stored at −20 °C. Neohydrin was obtained from ICN, K & K Lab, Inc. Stock solutions of 5 mM 4-(2-pyridylazo)resorcinol (PAR) were prepared as before (Hunt et al., 1985) and were stable for at least 1 month when stored at 4 °C in the dark in plastic containers. Dilutions of a 0.1000 M stock Zn^{2+} solution (Hunt et al., 1985) were prepared in 1 mM HCl on the day of use, and Zn^{2+} concentrations were checked by spectrophotometric titrations of 10^{-4} M PAR at 500 nm in pH 7.0 buffer and verified by atomic absorption measurements using standard Zn^{2+} in 5% nitric acid (Certified, Fisher Scientific) as the reference solution. Indo-1 (pentapotassium salt in sealed ampules) was obtained from Molecular Probes; stock solutions (~0.75 mM) were prepared by dissolving the contents of one ampule (~1 mg) in 1 mL of Chelex-treated buffer (pH 7.0), and concentrations were determined by UV absorbance from $\epsilon_{349nm} = 34 \times 10^3$ M^{-1} cm^{-1} (Grynkiewicz et al., 1986). Stock solutions (about 15 mM) of quin-2 were prepared by dissolving the solid in water while adding dilute KOH to maintain pH 11, and concentrations were determined by UV absorbance from $\epsilon_{261nm} = 37 \times 10^3$ M^{-1} cm^{-1} (Tsien, 1980). Stock solutions of indo-1 and quin-2 were divided and stored in plastic tubes at −20 °C; these were thawed only once for use. Quin-2 was diluted with buffer at pH 7.0, and the pH was adjusted to pH 7.0 (20 °C) if necessary. The purity of indo-1 and quin-2 was estimated to be >90% by fluorescence titrations with Zn^{2+} in which equivalency occurs at 1:1 Zn^{2+}:indicator. Also, solutions of PAR, indo-1, and quin-2 contained <1% metal ion impurities, as evidenced by absorbance changes upon addition of excess EDTA. All other chemicals were of analytical reagent grade.

Instrumentation. Polyacrylamide gel electrophoresis for characterization of proteins was performed by using either 7% running gel (with 1 cm of 3% stacking gel) and the Bio-Rad Protean slab gel unit (16-cm cell) as described before (Hunt et al., 1985) or a Pharmacia Phast system. A Radiometer Model 26 pH meter equipped with a Radiometer combined glass electrode type GK 2322C was used for pH measurements. A Perkin-Elmer Model 650-40 fluorometer was used for fluorescence measurements at 20 °C. Stopped-flow measurements were performed by using either the spectrophotometer described by Rhee and Chock (1976) or a Hi-tech Model SF-51 stopped-flow spectrophotometer/fluorometer. Atomic absorption analyses for Zn^{2+} were made by using a flame attachment to a Perkin-Elmer Model 630 spectrophotometer. Visible–UV spectrophotometric measurements were performed on a Perkin-Elmer Model 320 spectrophotometer with self-masking semimicrocuvettes of 1.00-cm path length. Temperatures of solutions and reference solutions were maintained at ±0.1 °C by circulated water through a thermostatable block. Second derivative spectra were obtained at 30 °C with a rapid-scan (diode array) UV–visible spectrometer (Hewlett-Packard Model 8450A) at ~0.1A_{280nm}, and each was the average of 60 spectra. CD spectra were obtained from 240 to 194 nm at 27 °C with a Cary Model 61 (0.2-degree scale with 0.5-nm slit) for 0.06–0.36 mg/mL r_2 in 0.10 M potassium phosphate, pH 7.2, and a cylindrical cell of 1.005-mm path length. The CD data were analyzed on an IBM PC using the CDEstimate program kindly provided by J. T. Yang at the University of California Medical School, San Francisco, CA (Yang et al., 1986). Calibrated thermistor probes were used to directly monitor solution temperatures. Buffer and protein solutions were degassed under vacuum before use to avoid interference from bubble formation during observations of absorbance, fluorescence, or CD changes.

Results

Kinetic measurements of Zn^{2+} release and uptake from isolated regulatory subunits (r_2) of ATCase first were made in order to obtain estimates of the affinity of r_2 for Zn^{2+} in the absence of stabilizing r–c contacts. Since these gave equivocal results, a second approach was used for the determination of the binding constant of r_2 for Zn^{2+} by rapid, steady-state spectral measurements of competition for Zn^{2+} between r_2 and indo-1 and between r_2 and quin-2. However, in order to calculate the binding constants of r_2 for Zn^{2+} from the latter data, it was necessary to determine the affinity constants of indo-1 and quin-2 for Zn^{2+} and also the spectral changes produced by Zn^{2+} binding to these indicators.[2]

Characterization of Isolated Regulatory Subunits of ATCase. Freshly isolated regulatory subunits routinely were titrated with PMPS in the presence of 10^{-4} M PAR. Any Zn^{2+} release to PAR prior to mercurial addition (≤30%) was attributed to free or loosely bound Zn^{2+} (due to the addition of excess Zn^{2+} to stabilize r_2 during its preparation; see Materials and Methods). The agreement between the concentration of r_2 obtained from A_{280nm} and mercurial-promoted Zn^{2+} release (1 Zn^{2+}/r chain) was used as a measure of the quality of the preparation of r dimer and was generally within ±10%. Because the mercurial-promoted release of Zn^{2+} from r_2 could be quantitated by formation of the highly absorbant $Zn(PAR)_2$ complex at 500 nm ($\Delta\epsilon = 6.6 \times 10^4$ M^{-1} cm^{-1}; Hunt et al., 1984, 1985), this was a 12-fold more sensitive measure of r_2

[2] Some properties of Zn^{2+} interactions with indo-1 and quin-2 at pH 7.0 and 20 °C, which were determined for the present study, are presented in Jefferson et al. (1990). For calculations, 1:1 complex formation between Zn^{2+} and indo-1 has $K'_A = (2.5 \pm 1.0) \times 10^{10}$ and $(6.2 \pm 0.5) \times 10^9$ M^{-1} and $\Delta\epsilon = (-2.4 \pm 0.2) \times 10^4$ at 367 nm and $(-2.1 \pm 0.2) \times 10^4$ M^{-1} cm^{-1} at 365 nm in the absence and presence of 100 mM KCl, respectively. For Zn^{2+} binding to quin-2, $K'_A = (9.4 \pm 3.3) \times 10^{11}$ and $(2.7 \pm 0.1) \times 10^{11}$ M^{-1} and $\Delta\epsilon = (-2.7 \pm 0.1) \times 10^4$ at 266 nm and $(-2.6 \pm 0.1) \times 10^4$ M^{-1} cm^{-1} at 265 nm in the absence and presence of 100 mM KCl, respectively.

concentration than that obtained from the 280-nm absorbance. In addition, r dimers were shown to be competent to combine with added catalytic trimers (c_3) by incubation of isolated r_2 with c_3 in a molar ratio of 3.0:2.1 for ~1 h at 30 °C, pH 7.0, followed by polyacrylamide gel electrophoresis as previously described (Subramani & Schachman, 1981; Hunt et al., 1985) to quantitate the ATCase (c_6r_6) formed.

The UV spectrum of r_2 was as shown by Nelbach et al. (1972) and is typical of that for a protein containing 3 Tyr, 5 Phe, and 0 Trp residues per r chain (Kim et al., 1987). The second derivative spectrum of r_2 in 0.10 M potassium phosphate, pH 7.2 was added to that of *N*-acetyl-L-tryptophanamide at pH 7 in a molar ratio of 3 Tyr to 1 Trp in order to apply the method of Ragone et al. (1984) for calculating the fractional extent of exposure of Tyr residues (α). This is possible because Trp contributions to the second derivative peak–trough values of interest are not influenced by the environment of Trp residues in proteins (Ragone et al., 1984). For the native r dimer containing 1 Zn^{2+}/r chain, $\alpha = 0.68$ from

$$\alpha = \frac{r_n - r_a}{r_u - r_a} \quad (1)$$

where each r value is the ratio of two peak–troughs centered at about (287–283 nm)/(295–291 nm) in the second derivative spectrum: $r_n = 1.21$ measured in this study for r chain in r_2 with 3 intrinsic Tyr and 1 extrinsic Trp added, and $r_u = 1.73$ and $r_a = 0.11$ for a Tyr/Trp molar ratio of 3:1 in 6 M guanidine hydrochloride and ethylene glycol, respectively, calculated from the data of Ragone et al. (1984). The value of α indicates that the equivalent of 2 of the 3 Tyr residues per r chain in r_2 are fully exposed to solvent. Using the same procedure with RNase A in 20 mM potassium phosphate, pH 7.0 buffer, an equivalent of 1.2 of the 6 Tyr residues in RNase A were found to be exposed to solvent. This result is consistent with X-ray structural data which show that all Tyr residues of this protein are partly constrained (Wyckoff et al., 1967).

CD spectral measurements from 240 to 194 nm were performed also for r dimer with 1 Zn^{2+} bound per r chain (see below) in 0.10 M potassium phosphate, pH 7.2. The far-UV CD spectrum of r_2 was comparable to that obtained for r_2 by Cohlberg et al. (1972). Analysis of our data by the program of Yang et al. (1986)[3] gave estimates of 14.5% helix, 49.5% β-structures, 2% turns, and 34% random structures, using a mean residue molecular weight of 111.8 (Kim et al., 1987). Thus, the r dimer containing 1 equiv of Zn^{2+}/r chain has predominantly β-structures and random structures in solution. This conclusion is in accord with the estimated fraction of tyrosyl residues exposed to solvent and with previous ORD results of Cohlberg et al. (1972).

Zn^{2+} Release and Uptake Measured in the Presence of PAR. Mercurial-promoted Zn^{2+} release from r dimer exactly corresponds to mercaptide formation during titration of isolated regulatory subunits with PMPS (Figure 1). Zn^{2+} release was measured by final absorbance increases at 500 nm in the presence of 10^{-4} M PAR. Mercaptide bond formation was measured at 250 nm in a separate titration of r_2 in the absence of PAR (Boyer, 1954; Hunt et al., 1984). The data of Figure 1 are normalized to the concentration of r dimer present, which was determined from the protein absorbance at 280 nm. The equivalence point from either data set occurred at 8.0 equiv

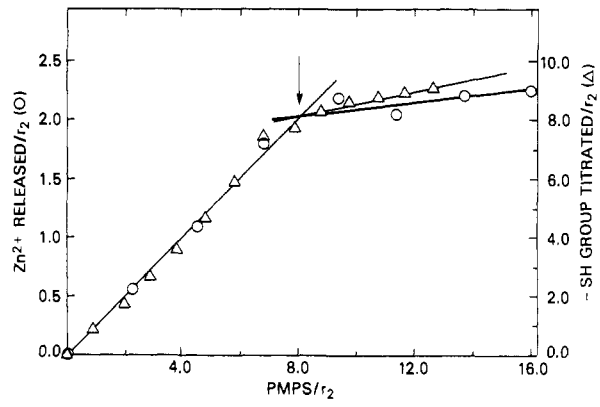

FIGURE 1: Correspondence of Zn^{2+} release and mercaptide bond formation on adding the mercurial reagent PMPS to r_2. Regulatory subunit (r_2) was titrated with PMPS at pH 7.0 and 20.0 °C. The final absorbance change was measured either at 250 nm (Δ) for –SH group reaction ($\Delta\epsilon = 3.9 \times 10^3$ M^{-1} cm^{-1}) or at 500 nm (O) for Zn^{2+} release in the presence of 10^{-4} M PAR ($\Delta\epsilon = 6.6 \times 10^4$ M^{-1} cm^{-1}; Hunt et al., 1984). Initial protein concentrations for the data given by Δ and O were 0.37 mg/mL (10.8 μM r_2) and 89 μg/mL (2.61 μM r_2), respectively, as determined from the protein absorbance at 280 nm (see Materials and Methods). Standardized solutions of PMPS were used. For ΔA_{250nm} data, 2-μL aliquots of 5.23 mM PMPS were added to r_2 in 1.00–1.026 mL of 40 mM Hepes, pH 7.0; for ΔA_{500nm} data, 10-μL aliquots of 6.56 mM PMPS were added to r_2 in 1.10–1.17 mL of 40 mM Hepes/100 mM KCl, pH 7.0. The arrow at 8.0 equiv of PMPS/r_2 gives the equivalence point for either data set.

of PMPS added per r dimer, at which point 2.0 equiv of Zn^{2+}/r_2 was released and all 8.0 –SH groups/r_2 had been titrated. This result is similar to that obtained with native ATCase (Hunt et al., 1984) and again indicates that once the first Zn^{2+}–sulfur bond in a Zn^{2+} binding cluster is broken, the other three –SH groups are more labile and therefore are both thermodynamically and kinetically more prone to form mercaptides than are –SH groups of intact Zn^{2+} binding sites. The small positive slopes at >8 PMPS/r_2 in Figure 1 are due to some interaction of the excess PMPS with PAR (circles) and the absorbance of PMPS itself at 250 nm (triangles).

Figure 2 illustrates stopped-flow measurements of the rates of PMPS-promoted Zn^{2+} release from r_2 (panel a) and of Zn^{2+} rebinding to r_2 after r_2-bound mercurial was displaced with excess 2-mercaptoethanol (panels b–d) in the presence of 10^{-4} M PAR. Representative oscilloscope traces obtained by averaging three to five mixing experiments are shown in Figure 2. In control experiments using the spectrophotometer, 100% of the Zn^{2+} bound to r_2 was released in the reaction of panel a and 80–90% of r_2 rebound Zn^{2+} in the reactions of panels b–d. Total absorbance changes accompanying these reactions in the stopped-flow experiments therefore can be estimated from the concentration of r and $\Delta\epsilon = 66\,000$ M^{-1}.

In Figure 2a, Zn^{2+} release from regulatory subunit was initiated by adding ~11-fold excess PMPS/–SH (taking into account the 2-ME present), and the transmittance decrease at 500 nm (inverted) as well as the first-order kinetic analysis[4] are shown. PMPS-promoted Zn^{2+} release from r_2 was first order with a half-time of ~50 ms at 15 °C and pH 7.0, and the same half-times (±4 ms) were obtained with >10-fold excess PMPS/–SH at 0.25 0.5, and 1.0 mM PMPS concentrations (data not shown). However, the measurements of Figure 2a were made in the presence of sulfate and phosphate anions which inhibit mercurial reactions (Khalifah et al.,

[3] When the CD analysis of Yang et al. (1986) was applied to CD data obtained for *E. coli* glutamine synthetase at pH 7.2, it was found to yield estimates of secondary structures that are in exact agreement with the X-ray data of David Eisenberg at UCLA (personal communication).

[4] In all cases, the same kinetic constants were obtained from analysis of transmittance or calculated absorbance changes at 500 nm in stopped-flow measurements.

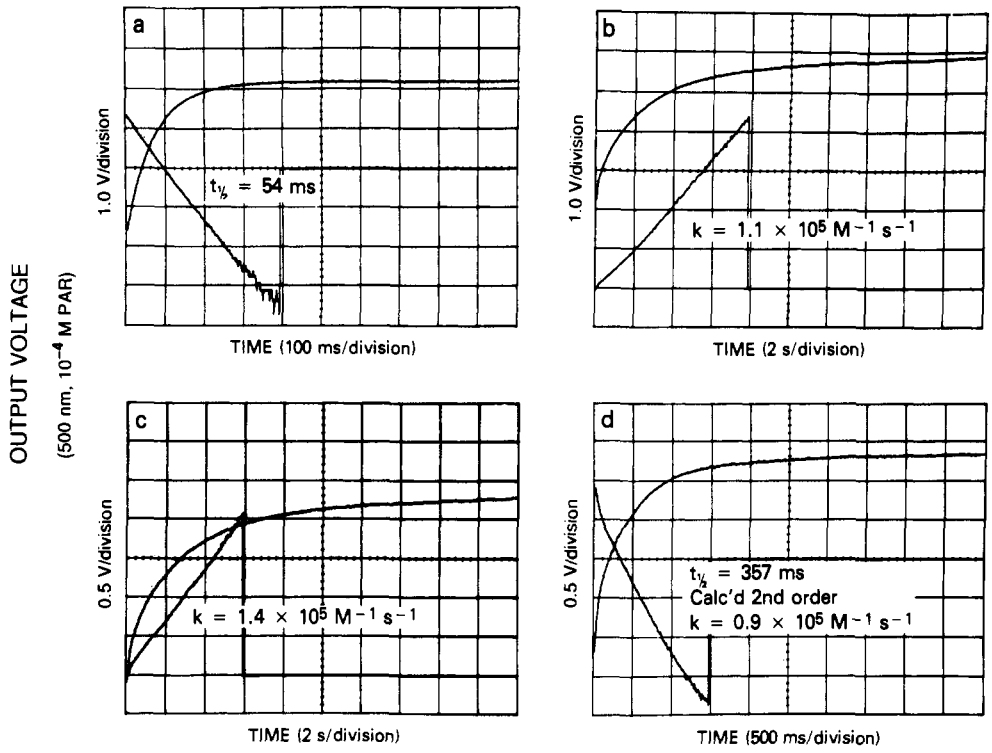

FIGURE 2: Stopped-flow measurements of Zn^{2+} release and apparent uptake at 15 °C in the presence of 10^{-4} M PAR and 40 mM potassium phosphate, pH 7.0. Just prior to measurements, regulatory subunits (r_2) were diluted 1:50 from 3.6 M $(NH_4)SO_4$–5 mM 2-ME with 40 mM potassium phosphate, pH 7.0, which also contained 1.1 equiv of PMPS per –SH group in panels b–d. Reactions (in 1:1 volume mixes) and final concentrations were as follows: 5.25 μM r chain + 0.8 mM PMPS in (a); 5.25 μM r–$(PMPS)_4$ and 6.4 μM Zn^{2+} + 10 mM 2-ME in (b); 3.0 μM r–$(PMPS)_4$ and 4.2 μM Zn^{2+} + 9.6 mM 2-ME and 2.9 μM c chain (as c_3) in (c); 5.25 μM r–$(PMPS)_4$ and 21.4 μM Zn^{2+} + 10 mM 2-ME in (d). Representative oscilloscope tracings (where y axis is output voltage proportional to transmittance changes of the stopped-flow apparatus) are shown for averages of at least 3 separate mixes recorded for PMPS-promoted Zn^{2+} release from r_2 (a) and for apparent Zn^{2+} uptake by apo-r_2 upon the displacement of the mercurial adduct of apo-r_2 by the addition of excess 2-ME (b–d). The upper tracings in a–d are records of photomultiplier output voltage (proportional to transmittance at 500 nm) as a function of time (inverted in panel a). Each tracing is comprised of 500 voltage–time data pairs recorded digitally at regular intervals. Lamp intensity and amplifier sensitivity were adjusted to give a difference of 10.0 V between 0 and 100% transmittance, so that absorbance values could be calculated from the relationship $A = -\log T = -\log (V/10) = 1 - \log V$. Infinite time voltage (V_∞) values could be estimated by retriggering the oscilloscope after ~30 s had elapsed (data not shown), but slow drifts caused by the high-intensity lamp made these unreliable. Consequently, V_∞ was treated as an adjustable parameter in iterative best fits of the data. The lower tracings in panels a and d are first-order rate plots, and those in panels b and c are second-order rate plots, generated by the computer of the stopped-flow apparatus. In the second-order analysis, total concentrations of r chain and Zn^{2+} were used as initial concentrations of the reactants. For the small absorbance changes occurring in these experiments, ΔA is proportional to ΔV, so that $(V_\infty - V_t)/(V_\infty - V_0)$ is the fraction of reactants remaining at time t.[4] For each analysis, the rate constant, or $t_{1/2}$ value, based on the linear portion of the rate plot, is shown.

1979). In the absence of inhibitory anions, the rate of mercurial-promoted Zn^{2+} release from r_2 is ~4.5-fold faster (Figure 4 below).

The stopped-flow traces of Figure 2b–d show transmittance increases at 500 nm when the mercurial adduct of r_2 in the presence of PAR–Zn^{2+} complexes was mixed with ~140-fold excess 2-ME (to mercurial) at 15 °C, pH 7.0. In Figure 2b, the Zn^{2+} present was equal to that released from r_2 by PMPS *plus* about 18% Zn^{2+} removed by PAR alone. A second-order analysis (inputting total [r] and total [Zn^{2+}] as the initial concentrations of the disappearing species and allowing the infinite time value of transmittance to vary in iterative fits) yielded a rate constant of 1.1 × 10^5 M^{-1} s^{-1} for the decrease in PAR–Zn^{2+} complexes, presumably equivalent to the rate of rebinding Zn^{2+} to aporegulatory subunits once 2-ME displaced the bound mercurial. The presence of nearly stoichiometric concentration of c chains in Figure 2c only increased the second-order k by 1.27-fold even though ATCase assembly occurs under these conditions as evidenced by polyacrylamide gel electrophoresis analysis [data not shown; see, for example, Hunt et al. (1985)]. This is consistent with catalytic subunits combining with regulatory subunits only after Zn^{2+} has been bound (Nelbach et al., 1972). The panel in Figure 2d shows an average of three stopped-flow traces obtained by adding excess 2-ME to the mercurial adduct of r_2 in the presence of a 4-fold excess of Zn^{2+} (chelated to PAR). Since this procedure relies on the transmittance increase due to disappearance of PAR–Zn^{2+}, this Zn^{2+} level was as high as could be attained and still measure a signal change. After ignoring the fast but small absorbance decrease produced by mixing 10 mM 2-ME with the highly absorbing Zn^{2+}–PAR mixture (due to 2-ME binding Zn^{2+}), the first-order analysis of the transmittance increase corresponding to the decrease in A_{500nm} yielded a calculated second-order k = 0.9 × 10^5 M^{-1} s^{-1} for Zn^{2+} binding to aporegulatory subunits.[4] This value is in good agreement with that measured in panel b of Figure 2 by second-order analysis when the Zn^{2+} present was 1.2-fold the concentration of r chain.

The experiments of Figure 2b,d were repeated in the presence of either 0.215 mM CTP or 0.10 mM ATP. At most, CTP or ATP increased the apparent second-order k about 1.3-fold for Zn^{2+} binding to apo-r_2.

In separate experiments (not shown), it became evident that 2-ME (a competing chelator of Zn^{2+}) had an accelerating effect on the rebinding of Zn^{2+} to apo-r_2 that was not simply related to the displacement of the PMPS bound to apo-r_2 subunits. Also, the possibility had to be considered that the 1:1 complex between PAR and Zn^{2+} and/or the ternary

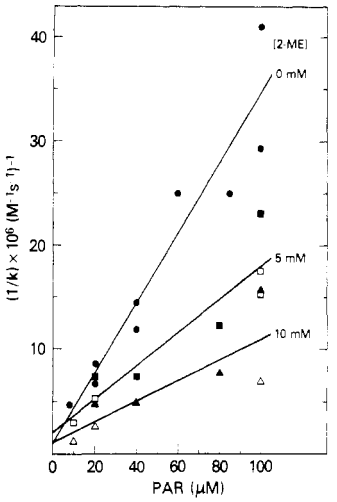

FIGURE 3: Second-order rates of apparent Zn^{2+} uptake by apo-r_2 at varying concentrations of PAR and 2-mercaptoethanol at pH 7.0 and 15 °C. Plots of the reciprocal of second-order rate constants measured in a stopped-flow apparatus (as in Figure 2b) for the binding of Zn^{2+} (5 μM) to apo-r_2 (3 μM r) in 40 mM potassium phosphate, pH 7.0 buffer as a function of [PAR] at the indicated fixed concentrations of 2-ME: Without 2-ME present (●), 5 mM 2-ME (■, □), and 10 mM 2-ME (▲, △). Regulatory subunit was mixed with Zn^{2+}·PAR complex (±2-ME) either as the reduced apoprotein (closed symbols) or as the mercaptide adduct of r_2 (open symbols). Reduced aporegulatory subunit was prepared by (a) passage of r_2 + PMPS through a Chelex (K^+ form) column to remove Zn^{2+} and free PMPS, (b) equilibration with excess 2-ME to displace protein-bound PMPS, and (c) passage through a P-10 column to remove 2-ME and 2-ME complexed to PMPS (see Materials and Methods). The mercurial adduct of r_2 was prepared by step a above. Protein prepared either by steps a–c or by step a only was used immediately in stopped-flow experiments. Solid lines are linear least square fits of all data at a given [2-ME].

complex composed of Zn^{2+}, PAR, and 2-ME was delivering Zn^{2+} to aporegulatory subunits since the rate of Zn^{2+} release from the 1:1 PAR–Zn^{2+} complex is slow, about 10^{-5} s^{-1} (Hunt et al., 1985). In an attempt to sort out these complex effects, aporegulatory subunits without bound mercurial were prepared and the apparent second-order rate of Zn^{2+} binding to r_2 was measured as functions of both 2-ME and PAR concentrations at 15 °C (Figure 3).

Plots of the reciprocal of the observed apparent second-order k values for Zn^{2+} uptake by apo-r_2 vs [PAR] at 0, 5, and 10 mM 2-ME concentrations are shown in Figure 3. An accelerating effect of 2-ME and an inhibition by PAR are indicated. However, linear fits of the data obtained at each 2-ME concentration as a function of [PAR] extrapolated to approximately the same $1/k$ value [$k = (8 \pm 3) \times 10^5$ M^{-1} s^{-1}] at zero [PAR]. Since 10^{-4} M PAR at pH 7.0 principally forms a 2:1 complex with Zn^{2+} (Tanaka et al., 1968), it is quite probable that the increasing apparent rate of Zn^{2+} uptake by apo-r_2 produced by decreasing [PAR] to concentrations less than 10^{-4} M is due to an increasing concentration of the 1:1 PAR–Zn^{2+} species. The total Zn^{2+} present as the 1:1 complex with PAR increases from ~2% at 100 μM PAR to ~15% at 10 μM PAR. The sulfhydryl reagent 2-ME also binds Zn^{2+}, although poorly, and it is possible that a ternary complex composed of 2-ME·PAR·Zn^{2+} facilitates delivery of Zn^{2+} to apo-r_2. Observe that the accelerating effect of 2-ME on the apparent rate of Zn^{2+} uptake by apo-r_2 shown in Figure 3 increases with increasing [PAR]; conversely, the effect of 2-ME effectively disappears as the data are extrapolated to zero [PAR]. However, 2-ME has little affect on the amplitude of the PAR signal for Zn^{2+} uptake by apo-r_2 (Hunt et al., 1985). Whatever the mechanism, it should not be forgotten

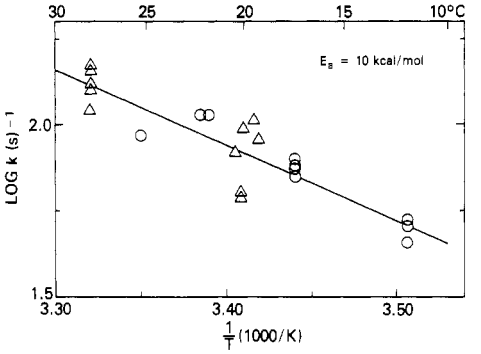

FIGURE 4: Arrhenius plot of the temperature dependence of first-order rate constants from stopped-flow measurements (High-Tech instrument) at 250 nm (○) or 500 nm (△) in the presence of 200 μM PAR on mixing regulatory subunit (r_2) with 10- to 20-fold excess PMPS per r_2–SH group. The buffer was 40 mM Hepes, pH 7.0 (at 20 °C), and 5.04 μM r chain ≡ 20.16 μM –SH or 2.55 μM r chain was mixed with an equal volume of 408 or 204 μM PMPS. To obtain first-order rate constants, the absorbance time data were collected continuously up to 0.1–0.25 s and were fit by means of a nonlinear least-squares program to the equation $A_t = (A_\infty - A_0)e^{-kt} + A_\infty$, where A_t, A_∞, and A_0 are the instantaneous time, infinite time, and initial time absorbances, respectively, k is the first-order rate constant, and t is the time in seconds. The computer program treats A_0, A_∞, and k as adjustable parameters and gives the best fit between absorbance–time data and the rate equation. Errors in computer fits were <5%. log k values for Zn^{2+} release (△) and mercaptide formation (○) vs $1/T$ (T in K) were fit by a linear least-squares program (solid line), and the Arrhenius activation energy (E_a) was calculated from the slope.

that the signal being monitored in these experiments is the decrease in the absorbance of the PAR·Zn^{2+} complexes corresponding to the disappearance of PAR·Zn^{2+} and not the appearance of the Zn^{2+}–protein complex.

In Figure 3, the same results were obtained by using either aporegulatory subunits with excess 2-ME present and adding Zn^{2+} or using the organomercurial–r_2 adduct and adding a solution containing both Zn^{2+} and excess 2-ME in the stopped-flow apparatus. Thus, the displacement of the mercurial from apo-r_2 by excess 2-ME was not rate limiting in the experiments of Figure 2b–d. The exchange of an organomercurial from one mercaptide linkage to another previously was estimated to occur with $k \cong 2 \times 10^7$ M^{-1} s^{-1} (Hunt et al., 1985).

The rates of Zn^{2+} release from r_2 and of mercaptide bond formation produced by the addition of 10- to 20-fold excess PMPS (per r_2–SH groups) were measured as a function of temperature at pH 7.0 in 40 mM Hepes buffer. An Arrhenius plot of these data is illustrated in Figure 4; the open triangles show data obtained at 500 nm in the presence of PAR, and the open circles show data obtained at 250 nm in the absence of PAR. Within experimental error, the rates for Zn^{2+} release upon adding excess PMPS to r_2 were the same as those for mercaptide bond formation. These results are similar to those obtained previously with ATCase (Hunt et al., 1984) and again indicate that PAR in the presence of mercurial has no active role in removing specifically bound Zn^{2+} from r_2 subunits. The tendency of r_2 to aggregate at >15 °C produced some scatter of the data and made it impossible to collect data at >30 °C; to demonstrate this fact, individual measurements (rather than averages) are shown from 12 to 28 °C in Figure 4. Nevertheless, it is apparent that the rates of mercurial-promoted release of Zn^{2+} from r_2 in Hepes buffer at pH 7.0 is rapid; a half-time of 9 ± 2 ms at 20 °C is indicated. The slope of the plot in Figure 4 gives an Arrhenius activation energy, E_a, = 10 kcal/mol. Although the rate of Zn^{2+} release from r_2 is 77-fold increased over that observed in the intact ATCase, the activation energy is about the same as that measured previously

for the mercurial-promoted Zn^{2+} release from ATCase with 100-fold excess PMPS when the -SH group of each catalytic chain was protected by the binding of *N*-(phosphonacetyl)-L-aspartate (Hunt et al., 1984).

Measurement of K'_A for Zn^{2+} Binding to r_2 with Indicators. The fluorescent Ca^{2+} probes synthesized by Tsien et al. (Tsien, 1980; Tsien et al., 1982; Grynkiewicz et al., 1985) are good spectrophotometric indicators for Zn^{2+} release from r_2 subunits of ATCase. Indo-1 and quin-2 compete directly with r_2 for Zn^{2+}, as shown by high absorbance difference spectra of panels A and C in Figure 5. The maximum decrease in the absorbance difference on Zn^{2+} binding occurs at 367 nm with indo-1 and at 266 nm with quin-2, so that the interference from protein and organic reagents with UV absorbances was greater with quin-2 than with indo-1. Most of the studies reported therefore were conducted with indo-1, even though quin-2 binds Zn^{2+} with a higher affinity than does indo-1.[2]

Curves 1–4 of Figure 5A show changes in the spectrum of ~20 μM indo-1 ($A_{350nm} \cong 0.7$) at pH 7.0 and 20 °C upon the addition of 0.59–2.05 μM r chain (as r_2) containing 1.27 equiv of Zn^{2+}. Maximum absorbance changes occur at 367 and 320 nm as Zn^{2+} from r_2 is chelated by indo-1. The duration of each scan was ~15 min, and no time-dependent absorbance changes were observed. Difference spectra for Zn^{2+} addition to indo-1 in the absence of protein has isosbestic wavelengths at 340, 284, and 233 nm, and that at 340 nm is evident also in the presence of r dimer. When 1.9-fold excess PMPS/-SH groups was added in Figure 5A (curve 5), all of the Zn^{2+} from r_2 was displaced to indo-1; the absorbance decrease at 367 nm was 111% of that calculated from the concentration of Zn^{2+} in r_2 and the $\Delta\epsilon$ value for indo-1 binding Zn^{2+}.[2] There was a small shift in the absorbance of indo-1 caused by some reaction of the mercurial with the indicator, as evidenced by a slight shift in the 340-nm isosbestic wavelength. When 2 μM $ZnCl_2$ was added after excess PMPS in an experiment not illustrated, ΔA_{367nm} was 103% of the expected value. The addition of a large excess of 2-ME/PMPS displaced PMPS from r_2 and allowed r_2 to rebind Zn^{2+} (Figure 5A, curve 6). When 100 μM EDTA was added to the sample after recording curve 6 of Figure 5A, a return to base line occurred, confirming the absence of metal ion contaminants in indo-1 solutions (data not shown). The maximum protein absorbance at 280 nm was only ~0.01 in Figure 5A whereas absorbance changes due to PMPS and mercaptide formation in curves 5 and 6 at <270 nm are more evident.

When 1.2 μM ATCase was added to ~70 μM indo-1 ($A_{350nm} \cong 2.4$), there was no significant change in the absorbance at 367 nm (curve 1 of Figure 5B). This is the expected result since Zn^{2+} release from ATCase requires mercurial attack (Nelbach et al., 1972). Curve 2 of Figure 5B was obtained 25 min after the addition of 3.6-fold excess of PMPs/-SH groups when time-dependent changes were complete (Hunt et al., 1984). The absorbance decrease at 367 nm in curve 2 was 111% of that calculated for complete Zn^{2+} release. Curve 3 of Figure 5B was recorded 15 min after the addition of a large excess of 2-ME and indicated that 75% of the Zn^{2+} was returned from indo-1 to protein. Once the mercurial was displaced from r_2 by 2-ME, Zn^{2+} could rebind to r_2 which then could associate with the c_3 subunits to reconstitute ATCase (Nelbach et al., 1972). If ATCase assembly is <100%, Zn^{2+} will redistribute between r_2 and indo-1 as in the experiments of Figure 5A, curves 1–4.

Figure 5C illustrates absorbance changes in ~40 μM quin-2 ($A_{261nm} \cong 1.5$; $A_{450nm} \cong 0.1$) at pH 7.0 and 20 °C. In contrast to experiments with indo-1 (Figure 5A), it was necessary to add regulatory subunits to both reference and sample cuvettes in the presence of quin-2 in order to compensate for protein absorbance changes. Since EDTA has been shown by Nelbach et al. (1972) to remove Zn^{2+} from r_2 subunits, the reference quin-2 solution was first treated with 0.3 mM EDTA (curve 1 in Figure 5C) and the apparent decrease in absorbance at 266 nm reflects the EDTA absorbance in the refrence cell. Then, 3.3 μM r chain (as r_2) containing about 12% excess Zn^{2+} was added to both cuvettes, and the absorbance decrease in curve 2 was recorded after 10 min at 20 °C; curve 3 was

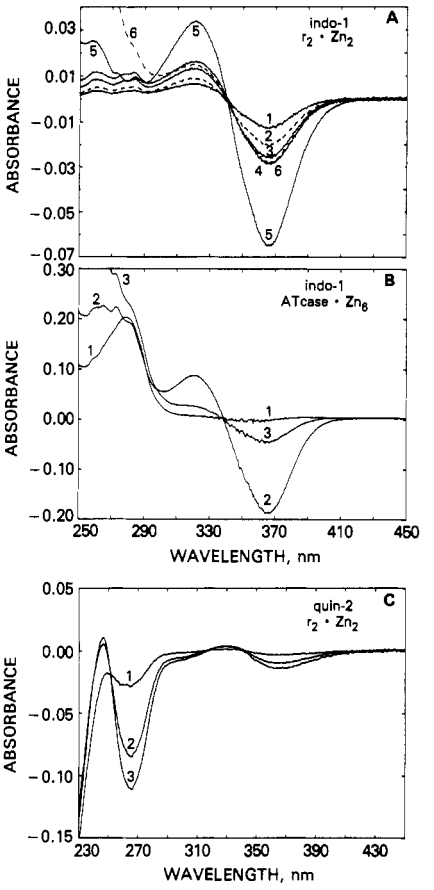

FIGURE 5: Reversible transfer of Zn^{2+} from regulatory subunits of ATCase to indo-1 (A, B) and to quin-2 (C) at pH 7.0 and 20 °C as evidenced by difference spectra. The sample and reference cells of the spectrophotometer contained the same concentration of indo-1 or quin-2 in 40 mM Hepes, pH 7.0. Protein in 40 mM Hepes, pH 7.0, and reagents were added to the sample cell in panels A and B and equal volumes of buffer were added to the reference cell in each case. In panel A (22–17 μM indo-1), curves 1–4 are difference spectra produced by four sequential additions of r_2: 0.59, 1.12, 1.60, and 2.05 μM r which contained 26.6% loosely bound Zn^{2+} (by PAR analysis; see Materials and Methods). After recording (4) in panel A, 15 μM PMPS (PMPS/r-SH = 1.9) was added, and (5) shows the complete release of Zn^{2+} from 2.02 μM r; the addition of 16 mM 2-ME to the sample in (5) produced (6), which shows that apo-r_2 then rebound Zn^{2+} to give the same trough at 367 nm as in (4). Absorbance increases at <290 nm in (5) and (6) of panel A are mainly due to mercaptide bond absorbance. In panel B (71–65 μM indo-1), the addition of 1.22 μM ATCase (with 4.5% loosely bound Zn^{2+}) produced (1); the subsequent addition of 128 μM PMPS gave (2) after 25 min for which 111% of the theoretical absorbance decrease at 367 nm for complete Zn^{2+} release from dissociated r_2 was obtained. Difference spectrum 3 in panel B was obtained after the addition of 9.2 mM 2-ME which gave 75% transfer of Zn^{2+} from indo-1 to r_2 which then could reassociate with c_3 subunits to reconstitute ATCase. In panel C (41.9–39.9 μM quin-2), EDTA (296 μM) was added to the reference cell (1) and then 3.34 μM r chain with 12% loosely bound Zn^{2+} (by PAR analysis) was added to both the sample and reference cells; difference spectra 2 and 3 were recorded at 20 °C, 10 min and 1 h (or after overnight incubation at 4 °C) later, respectively.

Table I: Relative Apparent Affinities ($K'_r/K'_{indo\text{-}1}$) of r Chain in r_2 and Indo-1 for Zn^{2+} at pH 7.0, 20 °C, in 40 mM Hepes/KOH Buffer[a]

$[indo\text{-}1]_{total}$ (μM)	$[r\ chain]_{total}$ (μM)	$[r\cdot Zn^{2+}]$ / $[indo\text{-}1\cdot Zn^{2+}]$[b]	$[r\ chain]_{free}$[b] (μM)	$K'_r/K'_{indo\text{-}1}$[c]
In the Absence of KCl				
21	0.59	0.48	0.33	30
20	1.12	0.78	0.45	33
19	1.60	0.96	0.53	33
18	2.05	1.28	0.48	46
69	2.08	0.29	1.57	12
66	2.37	0.77	1.14	43
35	2.91	1.40	0.65	72
29	3.79	1.74	0.75	64
66	3.96	0.79	2.05	25
61	6.49	1.38	2.22	36
				av 39 ± 18
In the Presence of 100 mM KCl				
40	1.38	2.36	0.34	275
71	6.49	3.24	0.86	261
33	8.62	4.13	1.03	125
38	16.80	5.99	0.92	230
48	16.85	6.40	0.78	373
				av 253 ± 89

[a] Calculated from data obtained as in Figure 5A. In each experiment, excess PMPS/r_2-SH was added as a control after the equilibrium measurements (see curve 5 of Figure 5A) and the absorbance change correspond within ±12% to that expected for the total amount of Zn^{2+} in r_2. [b] The concentration of indo-1·Zn^{2+} was calculated from $\Delta\epsilon = -2.4 \times 10^4$ at 267 nm and from $\Delta\epsilon = -2.1 \times 10^4\ M^{-1}\ cm^{-1}$ at 365 nm for indo-1 binding Zn^{2+} in the absence and presence of 100 mM KCl, respectively. The concentration of free r chain was obtained from [indo-1·Zn^{2+}] after correcting the latter value for free and/or loosely bound Zn^{2+} introduced with the protein and $[r\cdot Zn^{2+}] = [r\ chain]_{total} - [r\ chain]_{free}$; see text. [c] See eq 5.

obtained either after 1 h at 20 °C or after an overnight incubation at 4 °C. The time dependence of the absorbance decreases (with the main trough at 266 nm) is due to the slow removal of Zn^{2+} from r_2 by EDTA in the reference cell rather than a slow step in the release of Zn^{2+} from r_2 to quin-2 (see below).

Ratios of apparent affinity constants ($K'_r/K'_{indo\text{-}1}$) for r_2 binding Zn^{2+} to that for indo-1 binding Zn^{2+} at pH 7.0 (20 °C) are given in Table I. These values were calculated from the steady-state release of Zn^{2+} from r_2 to indo-1 in experiments similar to those shown in Figure 5A (curves 1–4). For the reaction

$$(r\cdot Zn^{2+})_2 + 2In \rightleftharpoons r_2 + 2(In\cdot Zn^{2+}) \quad (2)$$

the equilibria and equations in terms of the indicator (In) present forming a 1:1 complex with Zn^{2+} and one equivalent Zn^{2+} binding site per r chain in r_2 are

$$r + Zn^{2+} \overset{K'_r}{\rightleftharpoons} r\cdot Zn^{2+} \quad (3)$$

$$In + Zn^{2+} \overset{K'_{In}}{\rightleftharpoons} In\cdot Zn^{2+} \quad (4)$$

where K'_r is the apparent association constant for r chain in r_2 binding Zn^{2+} (assuming no interaction between Zn^{2+} binding sites in r_2 and no dissociation of apo-r_2 under the conditions of our experiments) and K'_{In} is the apparent constant for 1:1 complex formation between indicator (In) and Zn^{2+} determined under the same conditions as used for reaction 2.[2] Coupling reactions 3 and 4 gives

$$K'_r = K'_{In}\frac{[r\cdot Zn^{2+}][In]}{[In\cdot Zn^{2+}][r]} \quad (5)$$

where [In] and [r] are the free concentrations of indicator and r chain, respectively; [r·Zn^{2+}] and [In·Zn^{2+}] are concentrations of r chain and indicator complexed to Zn^{2+}, respectively.

Table II: Apparent Association Constants (K'_A) for r Dimer Binding Zn^{2+} in 40 mM Hepes/KOH, pH 7.0 at 20 °C, in the Absence and Presence of 100 mM KCl, Estimated Spectrally from Competition with Indo-1 and Quin-2[a]

chelating indicator	KCl present (mM)	no. of determinations	K'_A $(M\ r\ chain)^{-1}$
indo-1	0	13	1.1×10^{12}
indo-1	100	9	1.5×10^{12}
quin-2	0	1	1.9×10^{12}
quin-2	100	1	3.0×10^{12}
		$\sum = 24$	av $(1.3 \pm 0.6) \times 10^{12}$

[a] K'_A values are for r_2 binding Zn^{2+}, assuming no interactions between the two Zn^{2+} binding sites in r_2 and no dissociation of r_2 (see text).

(Note that writing the equilibria in eqs 3 and 4 in terms of $r_2\cdot Zn_2^{2+}$ implies incorrectly a dependence on the square of the Zn^{2+} concentration.)

The quantity of Zn^{2+}–indicator complex formed in reaction 2 was calculated from the absorbance decrease at 367 nm with indo-1 and at 266 nm with quin-2 in the absence of KCl (panels A and C, respectively in Figure 5). The Zn^{2+}–indicator complexes are formed by binding the loosely associated Zn^{2+} [12–30% of Zn^{2+} present in P-10 protein eluates as measured by reaction with PAR in the absence of added mercurial reagent (see Materials and Methods)] and in part by Zn^{2+} dissociation from high-affinity, specific Zn^{2+} binding sites in r_2 to form apo-r_2. The total concentration of r_2 added to the indicator was calculated from protein absorbance measurements at 280 nm and from the PMPS-promoted Zn^{2+} release from r_2 to PAR. Since 100 μM PAR removes loosely associated Zn^{2+}, the secondary Zn^{2+} binding sites of r_2 have a much lower affinity for Zn^{2+} than do indo-1, quin-2, or the thiol clusters of r_2. Under conditions of the binding measurements, therefore, 100% of the Zn^{2+} present is bound either to the indicator or to the thiol clusters of r_2. Subtracting the Zn^{2+} that is loosely bound to r_2 from the concentration of Zn^{2+}–indicator complex gives the amount of aporegulatory chains in eq 5. Subtracting the latter values from the total [r] in r_2 gives the quantity [r·Zn^{2+}] in eq 5.

The $K'_r/K'_{indo\text{-}1}$ ratios (eq 5) summarized in Table I were obtained with varying indo-1 and protein concentrations. The average relative affinity of r chain in r_2 for Zn^{2+} to that of indo-1 for Zn^{2+} is 39 ± 18 and 253 ± 89 in the absence and presence of 100 mM KCl, respectively. Within experimental error the $K'_r/K'_{indo\text{-}1}$ value was independent of the concentrations of indo-1 and r_2 over a 3-fold range of [indo-1] and an 11-fold range in protein concentration. These results indicate that r_2 does not interact with indo-1. The 6-fold increase in $K'_r/K'_{indo\text{-}1}$ produced by 100 mM KCl is due mainly to KCl decreasing the apparent affinity of indo-1 for Zn^{2+}.[2]

The apparent affinity constants for r dimer binding Zn^{2+} (K'_r) given in Table II were calculated from eq 5 by using averages of $K'_r/K'_{indo\text{-}1}$ ratios and the separately determined values of $K'_{indo\text{-}1}$ for indo-1 binding Zn^{2+} at pH 7.0 and 20 °C.[2] Similarly, experiments conducted with quin-2 (±KCl) were used to calculate K'_r values in Table II. Although only single determinations of $K'_r/K'_{quin\text{-}2}$ were made, the values of K'_r determined in the absence or presence of 100 mM KCl with indo-1 and quin-2 are very similar. The data of Table II give a best estimate of $K'_r = (1.3 \pm 0.6) \times 10^{12}\ M^{-1}$ (where the error is given as the standard deviation from the mean) for the binding of Zn^{2+} by r_2, assuming that the Zn^{2+} binding sites in r_2 are equivalent (noninteracting) and that apo-r_2 does not dissociate.

If apo-r_2 dissociates and apo-r binds Zn^{2+} with a much lower affinity than does apo-r_2, eq 5 becomes

$$K'_r = K'_{In}\frac{[r_2{\cdot}Zn^{2+}][In]}{K'_2[r]^2[In{\cdot}Zn^{2+}]} \quad (6)$$

where K'_2 is the apparent dimerization constant for apo-r_2 formation. Again, it is assumed that Zn^{2+} sites in r_2 are noninteracting and that zinc-containing r_2 does not dissociate. Cohlberg et al. (1972) found that $K'_2 \cong 10^4$ M^{-1} for EDTA-treated r_2 and $K'_2 > 10^7$ M^{-1} for $r_2{\cdot}Zn_2^{2+}$. From the value for $K'_2 = 10^4$ M^{-1} and the data of Table I, K'_r values of $(1.8 \pm 1.4) \times 10^{14}$ and $(2.4 \pm 1.6) \times 10^{14}$ M^{-1} in the absence and presence of 100 mM KCl, respectively, were calculated by eq 6. However, the applicability of eq 6 is questionable. As discussed below, apo-r_2 may not dissociate under the conditions of our experiments. Moreover, CTP was found by Cohlberg et al. (1972) to increase the dimerization constant K'_2 for apo-r_2 to $\sim 10^5$ M^{-1}, and yet 1 mM CTP had little or no effect on the distribution of Zn^{2+} between 1.4–8.4 μM r and excess indo-1 (data not shown).

The rate of transfer of Zn^{2+} from r dimer to quin-2 was estimated (with a 25-fold excess of quin-2/r chain) by monitoring the fluorescence signal with a 450-nm filter and excitation at 375 nm in a stopped-flow experiment. Since quin-2 has a small absorbance at $\geq$450 nm, inner-filter effects are negligible. When 310 μM quin-2 was mixed with 6 μM r dimer in 40 mM Hepes, pH 7.0 at 20 °C, the observed quench of emission took $\sim$10 s for completion. Unfortunately, the intense light source used with the stopped-flow apparatus causes some photodecomposition of the indicator over this time period. Consequently, it was necessary to correct the observed quench resulting from the mixing of quin-2 and r_2 for the fluorescence decay due to the indicator decomposition before first-order analysis. Nevertheless, an excellent first-order fit to the resultant quench data (an average of seven mixing experiments) was obtained. This analysis gave a first-order rate constant of $k = 0.36 \pm 0.01$ s^{-1} ($t_{1/2} = 1.9$ s) for the release of Zn^{2+} from r dimer at pH 7.0 and 20 °C in the presence of excess (0.3 mM) quin-2. This value is 1/210th of that observed for mercurial-promoted Zn^{2+} release from r_2 with 0.2–0.4 mM PMPS (Figure 4).

The effects of allosteric nucleotide effectors of ATCase on Zn^{2+} release from r_2 to excess indo-1 at pH 7.0 (20 °C) are shown schematically in Figure 6. The effects of ATP and CTP on the steady-state Zn^{2+} release from r_2 to indo-1 could be measured directly at $\sim$367 nm. Furthermore, the $\Delta\epsilon$ value at 368–365 nm for the addition of 1 mM $MgCl_2$ to indo-1 was only 0.4% of that for Zn^{2+}·indo-1 complex formation so that possible effects of added $MgCl_2$ could be tested also. CTP (1 mM $\pm$ 1 mM $MgCl_2$) or 1 mM Mg^{2+}·ATP increased the affinity of r_2 for Zn^{2+} by $\leq$1.2- or $\sim$1.9-fold, respectively. In contrast to the effect of Mg^{2+}·ATP, ATP alone had little effect on the Zn^{2+}–r_2 equilibrium. As already shown in Figure 5B, Figure 6 again illustrates that no Zn^{2+} was released from ATCase until PMPS addition and that a 3.6-fold excess of PMPS/–SH group produced 100% Zn^{2+} release from r_2 subunits of ATCase. The addition of excess 2-ME/PMPS allowed r_2 to rebind Zn^{2+} and, when equimolar c chains as c_3 subunits were present, $\sim$75% ATCase assembly occurred. The addition of excess c_3 subunits to r_2 produced less ATCase assembly in the absence than in the presence of 100 mM KCl. The response of r_2 to CTP and ATP appeared to be influenced by the presence of 100 mM KCl; however, in other experiments, CTP had no effect in the absence of KCl (see above) and the Mg^{2+} complexes of CTP and ATP were not tested in the presence of KCl. The experiments of Figure 6 are preliminary, but they do demonstrate that indo-1 can be used to study Zn^{2+} release from r_2 in the presence of KCl, mercurial, 2-ME, nucleotides, and c_3.

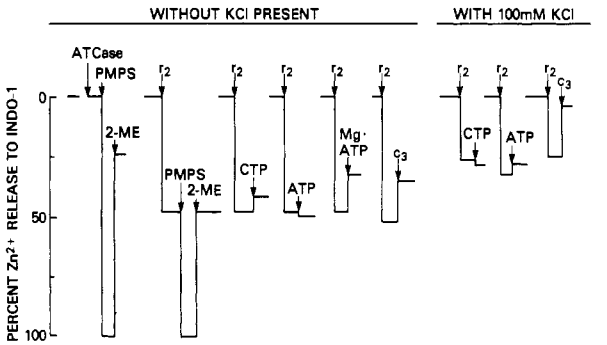

FIGURE 6: Schematic representation of the effect of nucleotides and other compounds on the percent release of Zn^{2+} from regulatory subunit (r_2) to indo-1 (66 μM) at 20 °C in 40 mM Hepes, pH 7.0. Protein concentrations were 1.2 μM ATCase or 1.2 μM r_2 except for the fifth r_2 addition shown when $r_2 = 2.1$ μM; the mercurial reagent PMPS produces complete Zn^{2+} release from ATCase and r_2. The sequence of additions is indicated, and final concentrations were 1.0 mM CTP or ATP ($\pm$1 mM $MgCl_2$), 22–130 μM PMPS, and 10 mM 2-ME; when isolated c_3 timer was added to r_2, c chain was 14.5 and 4.7 μM in the absence and presence of KCl, respectively.

Discussion

Zn^{2+} is the naturally occurring metal ion in *E. coli* ATCase (Rosenbusch & Weber, 1971a; Nelbach et al., 1972), and Zn^{2+} binding stabilizes the isolated r dimer (Cohlberg et al., 1972). Certainly, with 1 equiv of Zn^{2+} bound per 4 titratable –SH groups of each r chain in our preparations of the regulatory subunit (Figure 1), r_2 exists as a stable dimer. Also, there was a good correlation between the amount of tightly bound Zn^{2+} in r_2 preparations and their competency in ATCase assembly, for which the r dimer is required (Cohlberg et al., 1972). The instability of isolated apo-r_2 appears to be due primarily to the sensitivity of Zn^{2+} binding thiol clusters to air oxidation. In order to stabilize r_2 during its preparation, excess Zn^{2+} (200 μM) is added (Nelbach et al., 1972; Cohlberg et al., 1972; Yang et al., 1978), which results in Zn^{2+} binding to thiol clusters as well as to secondary sites. [For example, a value of 1.5 equiv of Zn^{2+} bound per r chain was measured for a preparation of r_2 at pH 7.0 containing 20 μM free Zn^{2+} (Shrake et al., 1981).] Since secondary sites of r_2 have a relatively low affinity for Zn^{2+}, these did not interfere with the measurements of this study; any Zn^{2+} bound to secondary sites of dialyzed r_2 (<30% of the total r_2-bound Zn^{2+}) could be quantitatively measured by its release to PAR and then taken into account in the equilibrium calculations with indo-1 and quin-2.

At neutral pH, r_2 is estimated to contain $\sim$50% β-structures, $\sim$34% random coil, and $\sim$15% α-helical structures from CD measurements made in the present study. Secondary structures for r chain in the T-form of intact ATCase is given as $\sim$30–34% β-structures and $\sim$18% α-helical structures from the X-ray crystallographic structural analysis of Kim et al. (1987). The greater percent of β-structures measured for isolated r_2 in potassium phosphate, pH 7.2, could reflect conformations free of the constraint of r chains in ATCase when r–c contacts are intact. In fact, Cohlberg et al. (1972) observed that the ORD and near-UV CD spectra of ATCase differed significantly from the sum of the isolated subunit contributions. Analysis of second derivative spectra of r_2 for the extent of tyrosyl exposure, which has been shown by Ragone et al. (1984) to correlate with X-ray structural analyses

of a variety of proteins, indicated that the equivalent of 2 of the 3 Tyr residues per r chain are fully exposed to solvent. This result is in complete agreement with the plots of thermal parameters (as an index of residue flexibility) for r chain in T-state ATCase (Kim et al., 1987). In the latter analysis, Tyr 77 and Tyr 89 would be expected to be exposed to solvent whereas Tyr 140 following Cys 138 is buried. Very low thermal parameters for the four Cys residues bonded to Zn^{2+} are given by Kim et al. (1987). However, the loop between residues 125 and 134 of r chain in ATCase appears to have some flexibility (Kim et al., 1987).

The present studies have been concerned mainly with the energetics and kinetics of Zn^{2+} interaction with isolated r_2 subunits of ATCase. Recently, the primary sequence around metal ion binding residues of several metalloproteins such as the regulatory subunits of ATCase, rubredoxin, and ferredoxin were found to be remarkably homologous to the "zinc finger" domain of transcription factor IIIA and related proteins that play important roles in eukaryotic systems of developmental and metabolic control through nucleic acid recognition (Berg, 1988). The proposed structure of Berg (1988), which consists of an antiparallel β-sheet followed by an α-helix, is based on detailed three-dimensional structures of the various metalloproteins.

An equilibrium constant $K'_A = (1.3 \pm 0.6) \times 10^{12}$ (M r chain)$^{-1}$ at pH 7.0 and 20 °C (corresponding to $\Delta G' = -16.2 \pm 0.3$ kcal/mol) has been determined for apo-r_2 binding Zn^{2+}, assuming noninteracting Zn^{2+} sites in r_2 and nondissociation of apo-r_2 (eq 5). This value for the affinity constant of r_2 for Zn^{2+} is within the expected magnitude since 0.4 mM EDTA removes Zn^{2+} from r_2 (Nelbach et al., 1972) and 0.1 mM PAR does not. The latter observations gave the estimate $10^{12} < K'_A < 10^{14}$ M^{-1} for Zn^{2+} binding to r_2 at pH 7.0 (Hunt et al., 1985). In order to measure an affinity constant of this magnitude with an unstable protein, competing metallochromic indicators were used to allow rapid steady-state equilibria to be established among r_2, apo-r_2, the Zn^{2+}–indicator complex, and free indicator. Indo-1 (Grynkiewicz et al., 1985) and quin-2 (Tsien, 1980) synthesized by Tsien and co-workers as fluorescent probes for Ca^{2+} have high affinities for Zn^{2+} and also are excellent spectrophotometric probes for Zn^{2+} (Jefferson et al., 1990). Neither indicator appeared to perturb the protein by interfering with the r_2–Zn^{2+} equilibria. Although the presence of 100 mM KCl substantially decreases the apparent affinities of indo-1 and quin-2 for Zn^{2+},[2] this concentration of KCl has little if any effect on the affinity of regulatory r dimer for Zn^{2+} (Table II).

The data of Cohlberg et al. (1972) indicate that prolonged EDTA treatment of regulatory subunits results in a monomer–dimer equilibrium (with a dimerization constant of $\sim 10^4$ M^{-1} and some nonparticipating higher aggregates). For the eventuality that apo-r_2 also dissociates under our rapid steady-state conditions, eq 6 is given. This yields a value for K'_A of $\sim 2 \times 10^{14}$ M^{-1}, when a dimerization constant of 10^4 M^{-1} and the data of Table I are used and it is assumed that Zn^{2+} binds with low affinity to r monomer and that Zn^{2+} sites in r dimer are noninteracting. However, a monomer–dimer equilibrium of apo-r_2 does not appear to be a significant factor in the present study, in which case eq 5 rather than eq 6 is applicable. The apparent K'_A value for r_2 binding Zn^{2+} in the presence of varying [indo-1] was independent of protein concentration in the range of 0.3–8.4 μM total r_2 (Table I). Furthermore, 1 mM CTP, which increases about 10-fold the dimerization constant for EDTA-treated apo-r_2 (Cohlberg et al., 1972), had little or no effect on the distribution of Zn^{2+} between 1.4–8.4 μM r and indo-1. The following observations should be recalled also. Time-dependent absorbance changes were not observed 5–120 min after adding r_2 to indo-1, and there was a return to the same equilibrium concentrations of r_2, apo-r_2, Zn^{2+}·indo-1, and indo-1 after sequential treatments with PMPS for complete Zn^{2+} release from r_2 and with excess 2-ME for Zn^{2+} rebinding to apo-r_2 (Figure 5A). Nonparticipating aggregates therefore did not form during this experiment. A single-order exponential for Zn^{2+} uptake by apo-r_2 was observed, but this only suggests that apo-r chains (if present) do not compete with apo-r_2 for Zn^{2+}.

The affinity of r_2 for Zn^{2+} was increased $\leq$1.2- and $\sim$1.7-fold by the binding of CTP and Mg·ATP, respectively. The effect of Mg^{2+} on ATP binding possibly has to do with charge neutralization by Mg^{2+} bound to β- and γ-phosphates of ATP, but this should be further explored. Interestingly, the effect of 1 mM CTP was the same in the absence and presence of 1 mM Mg^{2+}. A linkage between the free energies of Zn^{2+} and CTP binding was suggested by previous observations of Cohlberg et al. (1972) which showed that the affinity of r_2 for CTP was $\sim$10-fold that of the apoprotein. CTP and ATP, which are allosteric effectors of ATCase (Gerhart, 1970), bind in the flexible region of r chain well away from the Zn^{2+} domain but near r–r contacts in r_2 (Kim et al., 1987). However, Zn^{2+} domains are very near c–r contacts in intact ATCase, and these are enormously stabilized by the formation of nearby c–r chain contacts and accompanying conformational changes that occur during ATCase assembly. Chelators such as indo-1, quin-2, and EDTA cannot compete for Zn^{2+} in intact ATCase. Moreover, $^{65}Zn^{2+}$ does not exchange with Zn^{2+} bound to ATCase (Nelbach et al., 1972).

The experiments on the reaction between the aporegulatory subunits and Zn^{2+}–PAR were undertaken with the expectation that they would yield the rate of Zn^{2+} binding to apo-r_2. However, the most reasonable interpretation of the data for these experiments (Figure 3) is that we have instead studied the transfer of Zn^{2+} from $Zn(PAR)_1$ to apo-r_2, with the inverse dependence of the rate on [PAR] arising from the necessity of dissociating one PAR molecule from the dominant $Zn(PAR)_2$ to form a species that can react with the protein.[5] At equilibrium for 1×10^{-4} M PAR, $[Zn(PAR)_2]/[Zn(PAR)_1] \cong 20$. In the absence of 2-ME and with 10^{-4} M PAR, $k \cong 2.7 \times 10^4$ M^{-1} s^{-1} (Figure 3). Correcting for the factor of 20 leads to an estimate of $k = 5 \times 10^5$ M^{-1} s^{-1} for the second-order reaction of $Zn(PAR)_1$ with apo-r_2. This value is quite consistent with the value $k = (8 \pm 3) \times 10^5$ M^{-1} s^{-1} obtained by extrapolating the plot of $1/k$ vs [PAR] to [PAR] = 0 in Figure 3. If $Zn(PAR)_1$ is the active species, then as [PAR] is lowered, the apparent k should approach a limiting value which is the true k for the reaction of $Zn(PAR)_1$ with apo-r_2. The observed behavior and its interpretation are quite analogous to the results obtained by Tanaka et al. (1968) for the transfer of Zn^{2+} from $Zn(PAR)_2$ to EGTA, in which $Zn(PAR)_1$ was implicated as the active species for Zn^{2+} transfer. The direct transfer of Zn^{2+} between two multidentate chelating agents

[5] Although we have not been able to measure the rate constant for the reaction of apo-r_2 with free Zn^{2+}, we can set an upper limit of $\sim 1 \times 10^8$ M^{-1} s^{-1} for this constant; a larger value would make this pathway a major competitor (>50%) with the direct transfer of Zn^{2+} from Zn(PAR) to apo-r_2 in the experiments of Figure 3. We can use this maximum second-order k for Zn^{2+} association with apo-r_2 to set an upper limit also for the rate constant for the dissociation of Zn^{2+} from r_2, using our measured stability constant. Thus, $k_{dissociation} \leq (1 \times 10^8 \text{ M}^{-1} \text{ s}^{-1})/(1.3 \times 10^{12} \text{ M}^{-1}) \leq 0.8 \times 10^{-4}$ s^{-1} at pH 7.0 and 20 °C, which is at least 3 orders of magnitude slower than $k = 0.36$ s^{-1} observed for Zn^{2+} dissociation from r_2 in the presence of excess quin-2.

without the intermediate formation of "free" Zn^{2+} is undoubtedly what occurs in the living cell during the assembly of ATCase, since the plethora of natural chelating agents will make vanishingly small the concentration of "free" Zn^{2+}, by which we mean the complex with water, $Zn(H_2O)_6^{2+}$.

Inorganic chemists have studied extensively the kinetics and mechanisms of reactions in which metal ions are transferred between multidentate chelating agents. A summary of the data for such reactions in a review by Margerum et al. (1978) provides a background against which several of our observations can be better understood. In many cases the transfer of metal ions between chelating agents is more rapid than the reaction of the recipient chelator with the aquo complex of the metal. What seems to be necessary to start the transfer is an open coordination position on the metal to provide a toehold for the attacking ligand. Such an open position is provided more easily by the dissociation of a monodentate ligand, such as a water molecule, than by dissociation of one arm of a multidentate chelator. Once the transfer is started, with some arms of both chelators attached to the metal, the rest of the process resembles to a large extent the passing of a morsel of food from one octopus to another.

Under the conditions of our kinetic experiments we estimate [using stability constants of Tanaka et al. (1968)] that $Zn(PAR)_1$ is about 400 times as abundant as $Zn(H_2O)_6^{2+}$ in the presence of 10^{-4} M PAR. The $Zn(PAR)_1$ complex undoubtedly has one or more water molecules in addition to the dye coordinated to the metal, with the most likely composition being $Zn(PAR)(H_2O)_3$. The displacement of one of the waters by one of the sulfhydryl ligands of apo-r_2 would provide the needed toehold to begin the transfer of Zn^{2+}. This transfer results in the conversion of an octahedral Zn^{2+} complex to a tetrahedral complex, but such changes of geometry are facile for Zn^{2+} (Margerum et al., 1978). There is no reason to expect that the displacement of water from $Zn(H_2O)_6^{2+}$ would be much more rapid than from the $Zn(PAR)_1$ complex, as would be required to make the hexaaquo complex the active species. The enhancement by 2-ME of the rate of transfer of Zn^{2+} from PAR to the protein may be rationalized by assuming the formation of mixed complexes, such as $Zn(PAR)(2\text{-}ME)(H_2O)_2$, with 2-ME either enhancing displacement of water, acting as an efficient leaving group, or preventing a return to $Zn(PAR)_2$. Actually, 2-ME also was observed to have an accelerating effect on the observed rate of Zn^{2+} transfer from PAR to EDTA (Jefferson et al., 1987).

It is likely that the transfer of Zn^{2+} between r_2 and indo-1 or quin-2 is accomplished also by intermediates in which the protein and the dye are simultaneously bound to the metal, since equilibration is much more rapid than would be possible if $Zn(H_2O)_6^{2+}$ had to be formed as an intermediate.[5]

We now have in hand at least limited data on the release of Zn^{2+} from r_2 under three different conditions—namely, the spontaneous release to quin-2, the PMPS-promoted release to PAR, and the PMPS-promoted release to PAR when r_2 is part of the intact ATCase molecule. The PMPS-promoted release is much slower when r_2 is part of the intact ATCase molecule, but the activation energy is about the same as for the reaction of the mercurial with isolated r_2, so that the substantial difference in rates is an entropic effect. The less favorable entropy of activation for intact ATCase can probably be rationalized by the increased inaccessibility of the sulfhydryls to attack by the mercurial. The release of Zn^{2+} from the protein to quin-2 and the PMPS-promoted release are such different processes that a comparison of rates is nonsensical. It is likely that PMPS has an active role in effecting the cleavage of Zn–sulfur bonds, probably by electrophilic attack at sulfur, whereas quin-2 probably has to wait for a Zn–sulfur bond to cleave to provide an open coordination position on the Zn^{2+}.

Acknowledgments

We are indebted to Professor Howard K. Schachman at the University of California, Berkeley, CA, for encouraging this work and to Ying R. Yang in his laboratory for supplying preparations of purified ATCase which made this work possible. In addition, we thank Dr. Mark T. Fisher for measuring the second derivative spectrum of isolated regulatory subunits, Peter A. Cohen for performing CD measurements, and J. T. Yang for supplying the CDEstimate program for CD analysis of protein secondary structures (Yang et al., 1986).

Registry No. ATCase, 9012-49-1; Zn, 7440-66-6.

References

Berg, J. M. (1988) *Proc. Natl. Acad. Sci. U.S.A. 85*, 99–102.

Blackburn, M. N., & Schachman, H. K. (1976) *Biochemistry 15*, 1316–1323.

Boyer, P. D. (1954) *J. Am. Chem. Soc. 76*, 4331–4337.

Cohlberg, J. A., Pigiet, V. P., Jr., & Schachman, H. K. (1972) *Biochemistry 11*, 3396–3411.

Gerhart, J. C. (1970) *Curr. Top. Cell. Regul. 2*, 275–325.

Gerhart, J. C., & Pardee, A. B. (1962) *J. Biol. Chem. 237*, 891–896.

Grynkiewicz, G., Poenie, M., & Tsien, R. Y., (1985) *J. Biol. Chem. 260*, 3440–3450.

Han, M. K., Knutson, J., Kim, S. H., Fisher, M. T., Cyran, F. P., & Ginsburg, A. (1989) *Biophys. J. 55*, 120a.

Han, M. K., Cyran, F. P., Fisher, M. T., Kim, S. H., & Ginsburg, A. (1990) *J. Biol. Chem.* (in press).

Honzatko, R. B., Crawford, J. L., Monaco, H. L., Ladner, J. E., Edwards, B. F. P., Evans, D. R., Warren, S. G., Wiley, D. C., Ladner, R. C., & Lipscomb, W. N. (1982) *J. Mol. Biol. 160*, 219–263.

Hunt, J. B., Neece, S. H., Schachman, H. K., & Ginsburg, A. (1984) *J. Biol. Chem. 259*, 14793–14803.

Hunt, J. B., Neece, S. H., & Ginsburg, A. (1985) *Anal. Biochem. 146*, 150–157.

Jefferson, J. R., Hunt, J. B., & Ginsburg, A. (1987) *Fed. Proc., Fed. Am. Soc. Exp. Biol. 46* (6), 2047.

Jefferson, J. R., Hunt, J. B., & Ginsburg, A. (1988) *FASEB J. 2* (5), A1338.

Jefferson, J. R., Hunt, J. B., & Ginsburg, A. (1990) *Anal. Biochem. 187*, 328–336.

Kantrowitz, E. R., & Lipscomb, W. N. (1988) *Science 241*, 669–674.

Khalifah, R. G., Sanyal, G., Strader, D. J., & Sutherland, W. M. (1979) *J. Biol. Chem. 254*, 602–604.

Kim, K. H., Pan, Z., Honzatko, R. B., Ke, H., & Lipscomb, W. N. (1987) *J. Mol. Biol. 196*, 853–875.

Klug, A., & Rhodes, D. (1987) *Trends Biochem. Sci. (Pers. Ed.) 12*, 464–469.

Margerum, D. W., Cayley, G. R., Weatherburn, D. C., & Pagenkopf, G. K. (1978) Kinetics and Mechanisms of Complex Formation and Ligand Exchange, in *Coordination Chemistry* (Martell, A.E., Ed.) ACS Monograph 174, Vol. 2, pp 1–220, American Chemical Society, Washington, DC.

Meighen, E. A., Pigiet, V. P., Jr., & Schachman, H. K. (1970) *Proc. Natl. Acad. Sci. U.S.A. 65*, 234–241.

Miller, J., McLachlan, A. D., & Klug, A. (1985) *EMBO J. 4*, 1609–1614.

Monaco, H. L., Crawford, J. L., & Lipscomb, W. N. (1978) *Proc. Natl. Acad. Sci. U.S.A. 75*, 5276–5280.

Nelbach, M. E., Pigiet, V. P., Jr., Gerhart, J. C., & Schachman, H. K. (1972) *Biochemsitry 11*, 315-327.
Ragone, R., Colonna, G., Balestrieri, C., Servillo, L., & Irace, G. (1984) *Biochemsitry 23*, 1871-1875.
Rhee, S. G., & Chock, P. B. (1976) *Biochemsitry 15*, 1755-1760.
Rosenbusch, H. P., & Weber, K. (1971a) *J. Biol. Chem. 246*, 1644-1657.
Rosenbusch, J. P., & Weber, K. (1971b) *Proc. Natl. Acad. Sci. U.S.A. 68*, 1019-1023.
Shrake, A., Ginsburg, A., & Schachman, H. K. (1981) *J. Biol. Chem. 256*, 5005-5015.
Subramani, S., & Schachman, H. K. (1981) *J. Biol. Chem. 256*, 1255-1262.
Tanaka, M., Funahashi, S., & Shirai, K. (1968) *Inorg. Chem. 7*, 573-578.
Tsien, R. Y. (1980) *Biochemistry 19*, 2396-2404.
Tsien, R. Y., Pozzan, T., & Rink, T. J. (1982) *J. Cell. Biol. 94*, 325-334.
Weber, K. K. (1968) *Nature (London) 218*, 1116-1119.
Wyckoff, H. W., Hardman, K. D., Allewell, N. M., Inagami, T., Johnson, L. N., and Richards, F. M. (1967) *J. Biol. Chem. 242*, 3984-3988.
Yang, J. T., Wu, C.-S. C., & Martinez, H. M. (1986) *Methods Enzymol. 130*, 208-269.
Yang, Y. R., Kirschner, M. W., & Schachman, H. K. (1978) *Methods Enzymol. 51*, 35-41.

Vanadate Dimer and Tetramer Both Inhibit Glucose-6-phosphate Dehydrogenase from *Leuconostoc mesenteroides*†

Debbie C. Crans* and Susan M. Schelble
Department of Chemistry, Colorado State University, Fort Collins, Colorado 80523
Received January 8, 1990; Revised Manuscript Received April 5, 1990

ABSTRACT: Vanadate dimer and tetramer inhibit glucose-6-phosphate dehydrogenase from *Leuconostoc mesenteroides*. The inhibition by a vanadate mixture containing vanadate monomer, dimer, tetramer, and pentamer was determined by measuring the rates of glucose 6-phosphate oxidation and reduction of NAD (or NADP) catalyzed by glucose-6-phosphate dehydrogenase. The inhibition by vanadate is competitive with respect to NAD or NADP and noncompetitive (a mixed type) with respect to glucose 6-phosphate (G6P) when NAD or NADP are cofactors. This inhibition pattern varies from that observed with phosphate and thus suggests vanadate interacts differently than a phosphate analogue with the enzyme. ^{51}V NMR spectroscopy was used to directly correlate the inhibition of vanadate solutions to the vanadate dimer and/or tetramer, respectively. The activity of the vanadate oligomer varied depending on the cofactor and which substrate was being varied. The vanadate dimer was the major inhibiting species with respect to NADP. This is in contrast to the vanadate tetramer, which was the major inhibiting species with respect to G6P and with respect to NAD. The inhibition by vanadate when G6P was varied was weak. The competitive inhibition pattern with respect to NAD and NADP suggests the possibility that vanadate oligomers may also inhibit catalysis of other NAD- or NADP-requiring dehydrogenases. Significant concentrations of vanadate dimer and tetramer are only found at fairly high vanadate concentrations, so these species are not likely to represent vanadium species present under normal physiological conditions. It is however possible the vanadate dimer and/or tetramer represent toxic vanadate species.

Vanadium is an important dietary trace element that is beneficial at low concentrations (Nechay et al., 1986; Boyd & Kustin, 1984). At high concentrations vanadium becomes toxic. Vanadium is an insulin-mimetic agent and has cardiovascular activity (Gresser et al., 1987). It affects the cAMP levels, protein kinase activity, and protein phosphatase activity. The recent discovery of the vanadium-requiring nitrogenase is an example of the increasing interest in this element (Robson et al., 1986). The action of vanadium is likely to vary with the oxidation state of the metal although little is currently understood about the mechanisms of action of vanadium in mammals or plants. Vanadate [vanadium(V)] is the most stable form of vanadium in the presence of oxygen at neutral pH although reducing environments readily convert it to vanadium(IV) (Chasteen, 1983; Boyd & Kustin, 1984). Vanadium is generally believed to exist intracellularly in oxidation state IV, and vanadate is gradually reduced by endogenous reducing agents after being injected in the blood stream. However, in view of the presence of some free oxygen in the blood it seems possible that vanadium(IV) will reoxidize to vanadate. Recently, both vanadium(IV) and vanadium(V) were found bound to transferrin and albumin in blood serum (Chasteen et al., 1986). The nature of the oxidation state of vanadium (V(III) or V(IV)) in tunicate blood has been controversial and is now believed to be species dependent (Lee et al., 1988). In-depth understanding of the biological activities of vanadium is likely to require an understanding of the chemistry and biochemistry of both vanadium(IV) and vanadium(V).

The variety of effects of vanadium when normalizing the glucose levels in mammals may not be explained completely by the action of vanadium as an insulin-mimetic agent (Gresser et al., 1987). Recent studies show several biological effects of vanadate that are not observed with insulin (Bernier et al., 1988). Vanadium stimulates hexose transport, and this stim-

† This work was supported by the NIH (D.C.C.) and by an American Association of University Women (AAUW) fellowship (to S.M.S.).

0006-2960/90/0429-6698$02.50/0